Quasi-simultaneous two-band optical variability of the blazars 1ES 1959+650 and 1ES 2344+514

Haritma Gaur,[1,2]★ Alok C. Gupta,[1,2] A. Strigachev,[3] R. Bachev,[3] E. Semkov,[3] Paul J. Wiita,[4] S. Peneva,[3] S. Boeva,[3] N. Kacharov,[3,5] B. Mihov[3] and E. Ovcharov[5]

[1]*Aryabhatta Research Institute of Observational Sciences (ARIES), Manora Peak, Nainital 263129, Uttarakhand, India*
[2]*Department of Physics, DDU Gorakhpur University, Gorakhpur 273009, UP, India*
[3]*Institute of Astronomy and National Astronomical Observatory, Bulgarian Academy of Sciences, 72 Tsarigradsko Shosse Blvd, 1784 Sofia, Bulgaria*
[4]*Department of Physics, The College of New Jersey, PO Box 7718, Ewing, NJ 08628, USA*
[5]*Department of Astronomy, University of Sofia, 5 James Bourchier, 1164 Sofia, Bulgaria*

ABSTRACT

We report the results of quasi-simultaneous two-filter optical monitoring of two high-energy peaked blazars, 1ES 1959+650 and 1ES 2344+514, to search for microvariability and short-term variability (STV). We carried out optical photometric monitoring of these sources in an alternating sequence of *B* and *R* passbands, and have 24 and 19 nights of new data for these two sources, respectively. No genuine microvariability (intranight variability) was detected in either of these sources. This non-detection of intranight variations is in agreement with the conclusions of previous studies that high-energy peaked BL Lacs are intrinsically less variable than low-energy peaked BL Lacs in the optical bands. We also report the results of STV studies for these two sources between 2009 July and 2010 August. Genuine STV is found for the source 1ES 1959+650 but not for 1ES 2344+514. We briefly discuss possible reasons for the difference between the intranight variability behaviour of high- and low-energy peaked blazars.

Key words: galaxies: active – BL Lacertae objects: general – BL Lacertae objects: individual: 1ES 1959+650 – BL Lacertae objects: individual: 1ES 2344+514 – galaxies: photometry.

1 INTRODUCTION

Blazars constitute an enigmatic subclass of radio-loud active galactic nuclei (AGNs). Blazars include both BL Lacertae (BL Lac) objects and flat spectrum radio quasars, as both are characterized by strong and rapid flux variability across the entire electromagnetic spectrum. In addition, BL Lacs show largely featureless optical continua. Blazars exhibit strong polarization from radio to optical wavelengths and usually have core-dominated radio structures. According to the orientation-based unified model of radio-loud AGNs, blazar jets usually make an angle $\leqslant 10°$ to our line of sight (e.g. Urry & Padovani 1995). These extreme AGNs provide a natural laboratory to study the mechanisms of energy extraction from the central supermassive black holes and the physical properties of astrophysical jets.

The electromagnetic radiation from blazars is predominantly non-thermal. At lower frequencies [through the ultraviolet (UV) or X-ray bands] the mechanism is almost certainly synchrotron emission, while at higher frequencies the emission mechanism is probably due to inverse Compton (IC) emission (e.g. Sikora & Madejski 2001; Krawczynski 2004). The spectral energy distributions (SEDs) of blazars have a double-peaked structure (e.g. Giommi, Ansari & Micol 1995; Ghisellini et al. 1997; Fossati et al. 1998). Based on the location of the first peak of their SEDs, ν_{peak}, blazars are often subclassified into low-energy peaked blazars (LBLs) and high-energy peaked blazars (HBLs; Padovani & Giommi 1995). The first component peaks in the near-infrared/optical for LBLs and in the UV or X-rays for HBLs, while the second component usually peaks at GeV energies for LBLs and at TeV energies for HBLs.

Observations of blazars reveal that they are variable at all accessible time-scales, from a few tens of minutes to years, and even decades, at many frequencies (e.g. Carini & Miller 1992; Wagner & Witzel 1995; Gupta et al. 2004; Villata et al. 2007). These different time-scales allow the variability of blazars to be broadly divided into three classes, e.g. intraday variability (IDV), short-term variability (STV) and long-term variability (LTV). Variations in the flux of a source of a couple of hundredths of a magnitude up to a few tenths of magnitude over a time-scale of a day or less is known as IDV (Wagner & Witzel 1995) or microvariability or intranight optical variability. Flux changes observed over days to a few months are often considered to be STV, while those taking from several

★ E-mail: haritma@aries.res.in

months to many years are usually called LTV (e.g. Gupta et al. 2004).

For a better understanding of how the properties of HBLs relate to the previously known LBLs, we need to discriminate among the theoretical models that try to explain them. Optical observations offer a wealth of information on the variability of blazars. Over the past many years, a large amount of optical variability data for LBLs have been reported and rapid optical variability has been shown to be common (Rani et al. 2010, 2011, and references therein). However, because most of the HBLs were more recently found by X-ray and γ-ray sky surveys (Perlman et al. 2006; Abdo et al. 2010, and references therein) they have been less extensively monitored and the properties of the optical variability of HBLs are not yet clear. Preliminary observations of HBLs suggested that they show statistically lesser amounts of optical variability (Heidt & Wagner 1996, 1998) and polarized light than that of LBLs (Stocke et al. 1985, 1989; Jannuzi, Green & French 1993; Jannuzi, Smith & Elston 1994; Villata et al. 2000). Heidt & Wagner (1998) noticed that these objects likely display different duty cycles and variability amplitudes from those of the LBLs. Romero, Cellone & Combi (1999) found such differences in the case of microvariability, as just one out of three HBLs in their sample showed microvariations, while eight LBLs out of 12 did so. These differences were attributed to the possible presence of stronger magnetic fields in the high-energy peaked BL Lacs which could prevent the formation of small-scale jet inhomogeneities in these objects. However, due to the relative paucity of optical monitoring for HBLs, we cannot yet definitively say whether and how HBLs are different from LBLs in optical variability and therefore any additional high-quality observations of HBLs are particularly useful.

Here we report quasi-simultaneous observations of two HBLs, 1ES 1959+650 and 1ES 2344+514, in two optical bands (*B* and *R*) for the first time. In addition to looking for any microvariability in these two optical bands, our observations also give additional information on any microvariations in (*B* − *R*) colour. We also have searched for STV time-scales for these HBLs in the optical bands. We used five telescopes located in India, Bulgaria and Greece to monitor the optical variability of 1ES 1959+650 and 1ES 2344+514 between 2009 July and 2010 November.

The paper is structured as follows. In Section 2, we discuss the key features of these two HBLs. Section 3 describes the observations and data reduction procedure. Section 4 reports our results and we present our discussion and conclusions in Section 5.

2 PREVIOUS OBSERVATIONS

2.1 1ES 1959+650

One of the best studied members of the HBL subclass is 1ES 1959+650, with a redshift $z = 0.046$ (Véron-Cetty & Véron 2006). It was first detected at X-rays during the Slew Survey made by the *Einstein* satellite's Imaging Proportional Counter (Elvis et al. 1992). Based on the X-ray/radio versus X-ray/optical colour–colour diagram, the source was classified as a BL Lac object by Schachter et al. (1993). The mass of the central black hole (BH) in 1ES 1959+650 has been estimated to be $\sim 1.5 \times 10^8$ $M_\odot$ (Falomo, Kotilainen & Treves 2002).

Heidt et al. (1999) performed a detailed study of the optical band and found a complex structure composed of a luminous elliptical galaxy ($M_R = -23$) plus a disc and an absorption dust lane. Three photometric optical values were found in the literature, showing a great variation of the source brightness in the optical band. Its

brightness was reported as $V = 16$ by Marcha (1994); $V = 12.8$, as derived from digitalized plates, using $B - V = 0.5$ (Schachter et al. 1993); and an approximate magnitude of 13.67 obtained from the Cambridge Automatic Plate Measurement instrument (Perlman et al. 1996). Kurtanidze, Richter & Nikolashvili (1999) reported data taken during 1997–1999, finding brightnesses in the range $R = 14.50$–14.92. Krawczynski et al. (2004) carried out multiwavelength observations of strong flares from this source. Villata et al. (2000) observed the source from 1996 February 29 to 1997 May 30 and recorded a rapid decrease of 0.28 mag in 4 days. More recently, Ma et al. (2010) observed the source between 2003 May 4 and 2003 September 19 but saw no significant optical variations.

The blazar 1ES 1959+650 was further detected at X-rays with *ROSAT* and *BeppoSAX* (Beckmann et al. 2002). In 2002 May, the X-ray flux of the source had increased significantly. Both the Whipple (Holder et al. 2003) and High Energy Gamma Ray Astronomy (HEGRA) (Aharonian et al. 2003) collaborations subsequently confirmed a higher very high energy (VHE) γ-ray flux as well. Observing the source in 2000, 2001 and early 2002, the HEGRA collaboration yielded a marginal signal (Horns & Konopelko 2002).

An interesting aspect of the source activity in 2002 was the observations of a so-called 'orphan flare' (i.e. a flare of VHE γ-rays not accompanied by correlated increased activity at other wavelengths), recorded on June 4 by the Whipple Collaboration (Krawczynski et al. 2004; Daniel et al. 2005). The HEGRA collaboration had observed another, albeit less significant, orphan VHE signal during moonlight 2 days earlier (Tonello et al. 2003). Both of these flares in VHE γ-rays, observed in the absence of high activity in X-rays, are very difficult to reconcile with the standard synchrotron self-Compton model (Ghisellini et al. 1998), which is routinely very successfully employed to explain VHE γ-ray production. So, a hadronic synchrotron mirror model was proposed by Böttcher (2005) to explain this orphan TeV flare. 1ES 1959+650 was observed several times at TeV energies (Aharonian et al. 2003; Albert et al. 2006; Tagliaferri et al. 2008, and references therein), and unsurprisingly, this source is included in the first Fermi catalogue of AGNs (Abdo et al. 2010).

2.2 1ES 2344+514

This object, at $z = 0.044$, was identified as a BL Lac object (Perlman et al. 1996) and a 2-keV X-ray flux of 1.14 μJy was found while it had an optical brightness of $V = 15.5$ mag (with no galaxy subtraction). It was discovered in TeV γ-rays (>350 GeV) with the Whipple Observatory telescope and thus identified as a TeV BL Lac object (Catanese et al. 1998). Giommi, Padovani & Perlman (2000) reported rapid variability in the X-ray band on a time-scale of 5000 s. The VHE γ-ray emission from 1ES 2344+514 has been observed by the MAGIC collaboration (Albert et al. 2007) and Grube (2008) reported that this source showed a nightly variability in the integrated flux above 300 GeV.

Miller et al. (1999) observed 1ES 2344+514 and found a positive detection of optical microvariability, with a maximum range of about 0.08 mag over one night in the *V* band. Measurements in *R* band from 1998 September to 2000 October by Kurtanidze & Nikolashvili (2002) have shown LTV at the level of 0.1 mag; any IDV was confined within 0.05 mag and no evidence of microvariability at scales of hours or smaller was found. Dai et al. (2001) observed this source and reported a possible microvariation of 0.14 mag in the *V* band within 26 min, but the data quality was poor. Xie et al. (2002) monitored the source in 2000 and found no significant intraday variation (maximum flickering amplitudes are

Table 1. Details of telescopes and instruments.

Site	ARIES Nainital	NAO Rozhen	NAO Rozhen	AO Belogradchik	Skinakas Observatory, Crete
Telescope	1.04-m RC Cassegrain	2-m Ritchey–Chrétien	50/70 cm Schmidt	60-cm Cassegrain	1.3-m Modified RC
CCD model	Wright 2K CCD	PI VersArray:1300B	FLI PL160803	FLI PL09000	Andor DX436-BV-9CQ
Chip size (pixel)	2048×2048	1340×1300	4096×4096	3056×3056	2048×2048
Pixel size (μm)	24×24	20×20	9×9	12×12	13.5×13.5
Scale (arcsec pixel^{-1})	0.37	0.258	1.079	0.330^a	0.2825
Field (arcmin^2)	13×13	5.76×5.59	73.66×73.66	16.8×16.8	9.6×9.6
Gain (e$^-$ ADU^{-1})	10	1.0	1.0	1.0	2.687
Readout noise (e$^-$ rms)	5.3	2.0	9.0	8.5	8.14
Binning used	2×2	1×1	1×1	3×3	1×1
Typical seeing (arcsec)	1–2.8	1.5–3.5	2–4	1.5–3.5	1–2

^{a}With a binning factor of 1×1.

$\Delta V \sim 0.18$ mag and $\Delta R \sim 0.10$ mag) but, they did not find significant intraday variation because their errors on IDV light curve were ~ 0.05 mag. During observations in the *R* band in 2000 October no microvariability was observed (Fan et al. 2004). Ma et al. (2010) have claimed an optical variability amplitude in *R* band to be 0.69 ± 0.16 mag and time-scale to be 4 738 s, similar to the rapid variability of 5000 s noted earlier in the X-ray band, though this is presumably a coincidence.

3 OBSERVATIONS AND DATA REDUCTION

Observations of these two HBLs were performed using five optical telescopes, one in India, one in Greece and three in Bulgaria. All of these telescopes are equipped with CCD detectors and Johnson *UBV* and Cousins *RI* filters. Details of the telescopes, detectors and other parameters related to the observations are given in Table 1. A complete log of observations of these two HBLs from those five telescopes are given in Tables 2 and 3.

We carried out optical photometric observations during the period 2009 July to 2010 November. The raw photometric data were processed by standard methods that we now briefly describe. For image processing or pre-processing, we generated a master bias frame for each observing night by taking the median of all bias frames. The master bias frame for the night was subtracted from all flat and source image frames taken on that night. Then the master flat in each passband was generated by median combine of all flat frames in each passband. Next, the normalized master flat for each passband was generated. Each source image frame was flat-fielded by dividing by the normalized master flat in the respective band to remove pixel-to-pixel inhomogeneities. Finally, cosmic ray removal was done from all source image frames. Data pre-processing used the standard routines in Image Reduction and Analysis Facility[1] (IRAF) and ESO-MIDAS[2] softwares.

We processed the data using the Dominion Astronomical Observatory Photometry (DAOPHOT II) software to perform the circular concentric aperture photometric technique (Stetson 1987, 1992). For each night we carried out aperture photometry with four different aperture radii, i.e. $1 \times$ FWHM, $2 \times$ FWHM, $3 \times$ FWHM and $4 \times$ FWHM. On comparing the photometric results we found

that aperture radii of $2 \times$ FWHM almost always provided the best signal-to-noise ratio, so we adopted that aperture for our final results.

For these two HBLs, we observed three or more local standard stars on the same fields. The magnitudes of these standard stars are given in Table 4. We employed two standard stars from each blazar field with magnitudes similar to those of the target so as to not induce any significant errors due to differences in photon statistics. We used standard stars 4 and 6 for the blazars 1ES 1959+650 and stars C2 and C3 for the HBL 1ES 2344+514 and show their differential instrumental magnitudes for the IDV light curves. As the fluxes of the blazars and the standard stars were obtained simultaneously, and so at the same air mass and with identical instrumental and weather conditions, the flux ratios are considered to be very reliable. Finally, to calibrate the photometry of the blazars, we used the one standard star of each pair that had a colour closer to that of the blazar; star 6 and star C2 were the calibrators for 1ES 1959+650 and 1ES 2344+514, respectively. We adopted the magnitudes for these stars listed in Table 4 but did not incorporate the errors in their standardized magnitudes when quoting blazar magnitudes. Typical photometric errors for 1ES 1959+650 are ~ 0.01 mag in each of the *BVRI* bands, while for 1ES 2344+514 the errors in the *B* and *V* bands are ~ 0.02 mag while in the *R* and *I* bands it is ~ 0.01 mag.

4 RESULTS

4.1 Variability parameter detection techniques

Romero et al. (2002) pointed out how an inappropriate choice of the comparison stars used for differential photometry could result in spurious fluctuations in the differential light curve, and hence claims of spurious variability. To prevent this, we have selected non-variable or standard stars that closely match the target's magnitude and to be conservative we have removed isolated apparently discrepant points from our analysis. We have quantified our results by employing up to four different statistics (e.g. de Diego 2010). In our analysis, we have used standard stars 4 and 6 as stars A and B for 1ES 1959+650 and standard stars C2 and C3 as stars A and B for 1ES 2344+514.

4.1.1 C-test

The variability detection parameter, *C*, was introduced by Romero et al. (1999), and is defined as the average of *C*1 and *C*2 where

$$C1 = \frac{\sigma(BL - \text{star A})}{\sigma(\text{star A} - \text{star B})} \quad \text{and} \quad C2 = \frac{\sigma(BL - \text{star B})}{\sigma(\text{star A} - \text{star B})}. \quad (1)$$

Table 2. Observation log of optical photometric observations of 1ES 1959+650.

Date of observation (yyyy mm dd)	Telescope	Data points filters (B, V, R, I)
2009 07 23	B	1,1,1,1
2009 07 26	D	56,2,56,2
2009 07 27	D	58,1,58,1
2009 07 28	D	57,1,57,1
2009 07 29	D	56,2,55,2
2009 07 30	D	76,1,37,1
2009 08 03	E	42,2,43,2
2009 08 05	E	102,2,102,2
2009 08 17	D	57,1,56,1
2009 08 20	D	50,2,49,2
2009 08 21	D	62,2,61,2
2009 08 27	E	90,2,90,2
2009 09 22	C	90,2,90,2
2009 10 03	E	65,2,67,2
2009 10 09	A	1,1,81,1
2009 10 10	A	1,1,1,1
2009 11 13	D	2,2,2,2
2009 11 14	D	2,2,2,2
2009 11 16	C	2,2,2,2
2009 11 17	C	2,2,2,2
2009 11 19	C	2,2,2,2
2009 11 20	C	2,2,2,2
2009 11 21	C	2,2,2,2
2009 11 25	B	2,2,2,2
2010 05 09	C	3,2,96,4
2010 05 13	C	2,2,2,2
2010 06 08	C	2,2,2,2
2010 06 10	C	2,2,2,2
2010 06 12	C	2,2,2,2
2010 06 19	E	61,2,61,2
2010 07 15	D	20,2.19,2
2010 07 16	D	32,2,32,2
2010 07 17	E	78,2,78,2
2010 07 17	C	2,2,80,2
2010 07 19	E	62,2,62,2
2010 07 21	E	72,2,72,2
2010 08 05	D	21,2,21,2
2010 08 06	C	2,2,2,2
2010 08 07	C	2,2,2,2
2010 08 08	C	2,2,2,2
2010 08 09	C	2,2,2,2
2010 08 10	D	15,1,15,1
2010 11 04	C	2,2,2,2
2010 11 05	C	2,2,2,2

Table 3. Observation log of optical photometric observations of 1ES 2344+514.

Date of observations (yyyy mm dd)	Telescope	Data points filters (B, V, R, I)
2009 07 23	B	1,1,1,1
2009 08 04	E	52,2,52,2
2009 08 18	D	45,8,41,8
2009 08 19	D	42,6,40,6
2009 08 21	C	1,1,1,1
2009 08 22	C	36,1,36,1
2009 08 25	C	44,2,44,2
2009 08 26	E	46,3,48,3
2009 08 28	C	45,2,46,2
2009 08 29	C	54,2,54,2
2009 09 18	E	42,2,42,2
2009 09 21	C	29,1,32,2
2009 10 03	E	32,2,32,2
2009 10 10	A	1,1,65,1
2009 11 13	D	2,2,2,2
2009 11 14	D	2,2,2,2
2009 11 16	C	2,2,2,2
2009 11 17	C	2,2,2,2
2009 11 19	C	2,2,2,2
2009 11 20	C	2,2,2,2
2009 11 21	C	2,2,2,2
2009 11 25	B	2,2,2,2
2010 01 10	A	1,1,49,1
2010 01 11	A	1,1,50,1
2010 01 20	A	1,1,30,1
2010 06 09	C	2,2,2,2
2010 06 11	C	2,2,2,2
2010 06 13	C	2,2,2,2
2010 07 18	C	2,2,114,2
2010 07 18	E	62,4,62,4
2010 07 20	E	86,2,86,2
2010 07 22	E	17,2,17,2
2010 08 06	C	2,2,2,2
2010 09 08	C	2,2,2,2
2010 09 09	C	2,2,2,2
2010 10 31	C	2,2,2,2
2010 11 01	C	2,2,2,2
2010 11 04	C	2,2,2,2
2010 11 05	C	2,2,2,2
2010 11 06	C	2,2,2,2

A: 1.04-m Sampuranand Telescope, ARIES, Nainital, India.
B: 2-m Ritchey–Chretien Telescope at National Astronomical Observatory, Rozhen, Bulgaria.
C: 50/70 cm Schmidt Telescope at National Astronomical Observatory, Rozhen, Bulgaria.
D: 60-cm Cassegrain Telescope at Astronomical Observatory Belogradchik, Bulgaria.
E: 1.3-m Skinakas Observatory, Crete, Greece.

Here $(BL - star\ A)$ and $(BL - star\ B)$ are the differential instrumental magnitudes of the blazar and standard star A, and the blazar and standard star B, respectively, while $\sigma(BL - star\ A)$, $\sigma(BL - star\ B)$ and $\sigma(star\ A - star\ B)$ are the observational scatters of the differential instrumental magnitudes of the blazar and star A, the blazar and star B, and star A and star B, respectively. If $C \geq 2.576$, the nominal confidence level of a variability detection is >99 per cent, and we follow much of the previous literature (Jang & Miller 1997; Stalin et al. 2004 ; Gupta et al. 2008) in considering this to be a positive detection of a variation. However, this C-test is not a true statistic as it is not appropriately distributed and this criterion is usually too conservative (de Diego 2010).

4.1.2 F-test

We test our variability results using the standard F-test, which is a properly distributed statistic (de Diego 2010). Given two sample variances such as s_Q^2 for the blazar instrumental light-curve measurements and s_*^2 for that of the standard star, we have

$$F = \frac{s_Q^2}{s_*^2}. \tag{2}$$

Table 4. Standard stars in the blazar fields.

Source name	Standard star	B magnitude[a] (error)	V magnitude (error)	R magnitude (error)	I magnitude[a] (error)	References
1ES 1959+650	1	13.37 (0.02)	12.67 (0.04)	12.29 (0.02)	11.92 (0.01)	1, 3
	2	13.45 (0.02)	12.86 (0.02)	12.53 (0.02)	12.22 (0.01)	1, 3
	3	14.93 (0.02)	13.18 (0.02)	12.27 (0.02)	11.37 (0.01)	1, 3
	4	15.28 (0.02)	14.53 (0.03)	14.08 (0.03)	13.62 (0.01)	1, 3
	5	15.60 (0.03)	14.54 (0.03)	14.00 (0.02)	13.36 (0.02)	1, 3
	6	15.97 (0.02)	15.20 (0.03)	14.78 (0.03)	14.37 (0.01)	1, 3
	7	16.01 (0.02)	15.24 (0.03)	14.79 (0.03)	14.37 (0.01)	1, 3
1ES 2344+514	C1	–	12.61 (0.04)	12.25 (0.04)	11.90 (0.04)	2
	C2	–	14.62 (0.06)	14.20 (0.05)	13.84 (0.04)	2
	C3	–	15.89 (0.08)	15.40 (0.08)	14.89 (0.08)	2

1. Villata et al. (1998); 2. Fiorucci, Tosti & Rizzi (1998).
[a]3. Doroshenko et al. (2007).

The number of degrees of freedom for each sample, ν_Q and ν_*, will be the same and equal to the number of measurements N minus 1 ($\nu = N - 1$). The F value is then compared with the $F_{\nu_Q, \nu_*}^{(\alpha)}$ critical value, where α is the significance level set for the test. The smaller the α value, the more improbable the result produced by chance is. If F is larger than the critical value, the null hypothesis (no variability) is discarded. We have performed F-test at two significance levels (0.1 and 1 per cent) which correspond to 3σ and 2.6σ detections, respectively.

4.1.3 χ^2 test

We also performed a χ^2 test on the data. Given a number of observations of a source over a given period of time, the χ^2 statistic is expressed by

$$\chi^2 = \sum_{i=1}^{N} \frac{(V_i - \overline{V})^2}{\sigma_i^2}, \tag{3}$$

where $\overline{V}$ is the mean magnitude and the ith observation yields a magnitude V_i with a corresponding standard error σ_i. Here σ_i is the expected error, the error from considering photon noise from the source and sky, along with the CCD readout and all possible non-systematic sources of error. Since such errors are often calculated from the usually underestimated values yielded by the IRAF reduction package, an error rescaling is necessary. Usually, theoretical errors are smaller than the real errors by a factor of typically 1.3–1.75 (e.g. Gopal-Krishna et al. 2003; Bachev, Strigachev & Semkov 2005; Gupta et al. 2008). Our analysis of the current data indicates that this value is, on average, ∼1.5. So the errors that the program codes return should be multiplied by 1.5 to get better estimates of the real errors of the photometry. This statistic is compared against a critical value $\chi_{\alpha, \nu}^2$ obtained from the χ^2 probability function, where α is again the significance level and $\nu = N - 1$ are the degrees of freedom. If $\chi^2 > \chi_{\alpha, \nu}^2$ the test indicates a larger than expected scattering of the data points, and hence evidence of variability.

4.1.4 ANOVA test

ANOVA tests are used to compare the means of a number of samples. de Diego et al. (1998) used the one-way ANOVA test to investigate the variability in the light curves of quasars. This method consists of measuring k groups of $n_j = 5$; in short cadence observations such as ours, these groups should be ideally separated by 20–30 min. Variance of the means of each group of five observations and the mean for the dispersion within the groups are computed.

Then, the ratio between these variances is calculated and multiplied by the number of observations in each group. The number obtained behaves as the F-statistic and we compare the F-value with the critical values $F_{\nu_1, \nu_2}^{(\alpha)}$. In this test, if N is the number of observations and k is the number of groups ($k = N/n$), the number of degrees of freedom are $\nu_1 = k - 1$ for the groups and $\nu_1 = N - k$ for the errors; therefore, $\nu_1 + \nu_1 = N - 1$ corresponds to the degrees of freedom of the original data set. For a certain significance level α, if F exceeds the critical value, the null hypothesis will be rejected. We have used the inbuilt ANOVA code available in R.

4.1.5 Variability amplitude

Heidt & Wagner (1996) introduced the variability amplitude, defined as

$$A = \frac{100}{\langle A \rangle} \sqrt{(A_{\max} - A_{\min})^2 - 2\sigma^2} \text{ (per cent)}, \tag{4}$$

where $A_{\max}$ and $A_{\min}$ are the maximum and minimum fluxes in the calibrated LCs of the blazar, $\langle A \rangle$ is their mean, and the average measurement error of the blazar light curve (LC) is σ. We use this approach to quantify any variability.

4.2 Results for intraday variability

4.2.1 1ES 1959+650

We observed the source 1ES 1959+650 on 21 nights (quasi-simultaneously in optical bands B and R) and three nights in the R band alone from 2009 July to 2010 August for microvariability. We have performed the four tests discussed above on these data. The C, F, χ^2 and ANOVA parameters never exceed the 99 per cent confidence level (Table 5) for B, R or (of course) $(B - R)$. So this source was stable with respect to IDV during our observations. The differential light curves of the source are given in Figs 1 and 2 for these 24 nights.

4.2.2 1ES 2344+514

We observed the source 1ES 2344+514 on 14 nights (quasi-simultaneously in the B and R bands) and five nights in the R band from 2009 August to 2010 July for microvariability. We have tested for IDV using all four tests but no positive results were ever obtained in the B, R or $(B - R)$ bands as the C, F, χ^2 and ANOVA results never showed significance levels above 99 per cent considering both stars (Table 6); although several F-test values exceed 0.99

Table 5. Results of intraday variability observations of 1ES 1959+650.

Date	Band	N	C-test C_1, C_2	F-test $F_1, F_2, F_c(0.99), F_c(0.999)$	χ^2 test $\chi_1^2, \chi_2^2, \chi_{0.99}^2, \chi_{0.999}^2$	ANOVA $F_1, F_2, F_c(0.99), F_c(0.999)$	Variable
26.07.09	B	55	0.76, 1.02	0.57, 1.04, 1.90, 2.36	29.17, 18.20, 81.07, 91.87	1.33, 3.30, 2.75, 3.78	NV
	R	56	0.48, 0.96	0.23, 0.92, 1.89, 2.34	94.25, 89.98, 82.29, 93.16	0.92, 3.91, 2.75, 3.78	NV
	$(B - R)$	55	0.79, 0.78	0.63, 0.96, 1.90, 2.36	28.60, 20.94, 81.07, 91.78	1.18, 1.30, 2.75, 3.78	NV
27.07.09	B	58	0.86, 0.85	0.73, 0.72, 1.87, 2.30	22.31, 24.06, 84.73, 95.75	0.79, 2.31, 2.66, 3.62	NV
	R	58	0.88, 1.09	0.77, 1.19, 1.87, 2.30	30.45, 19.58, 84.73, 95.75	0.69, 3.30, 2.66, 3.62	NV
	$(B - R)$	58	0.89, 0.82	0.80, 0.66, 1.87, 2.30	18.95, 23.79, 84.73, 95.75	0.85, 1.57, 2.66, 3.62	NV
28.07.09	B	51	0.91, 0.83	0.83, 0.68, 1.95, 2.44	17.43, 21.84, 76.15, 86.66	0.99, 1.22, 2.89, 4.02	NV
	R	57	0.98, 0.94	0.96, 0.88, 1.88, 2.32	19.08, 21.29, 83.51, 94.46	2.10, 3.37, 2.75, 3.78	NV
	$(B - R)$	51	0.91, 0.82	0.83, 0.67, 1.95, 2.44	19.15, 24.50, 76.15, 86.66	1.02, 1.11, 2.89, 4.02	NV
29.07.09	B	54	0.74, 0.88	0.55, 0.78, 1.91, 2.38	25.96, 19.05, 79.84, 90.57	1.47, 0.51, 2.76, 3.80	NV
	R	51	0.75, 0.89	0.56, 0.80, 1.95, 2.44	23.67, 17.62, 76.15, 86.66	1.98, 2.85, 2.89, 4.02	NV
	$(B - R)$	53	0.69, 0.79	0.47, 0.62, 1.92, 2.40	21.59, 17.33, 78.62, 89.27	0.82, 0.25, 2.89, 4.02	NV
30.07.09	B	33	0.88, 0.79	0.77, 0.62, 2.32, 3.09	15.41, 21.59, 53.49, 62.49	1.07, 2.58, 3.90, 5.98	NV
	R	36	1.02, 0.94	1.03, 0.88, 2.23, 2.93	12.02, 14.14, 57.34, 66.62	2.91, 0.57, 3.53, 5.24	NV
	$(B - R)$	34	0.65, 0.78	0.43, 0.60, 2.29, 3.04	29.43, 22.30, 54.78, 63.87	0.70, 0.58, 3.56, 5.31	NV
03.08.09	B	42	0.74, 0.65	0.55, 0.42, 2.09, 2.69	30.37, 39.63, 64.95, 74.74	4.63, 2.59, 3.26, 4.72	NV
	R	42	0.81, 0.74	0.65, 0.55, 2.09, 2.69	18.80, 22.45, 64.95, 74.74	0.66, 1.57, 3.26, 4.72	NV
	$(B - R)$	42	0.73, 0.63	0.53, 0.40, 2.09, 2.69	37.65, 49.91, 64.95, 74.74	4.15, 2.13, 3.26, 4.72	NV
05.08.09	B	102	0.84, 0.83	0.70, 0.68, 1.59, 1.86	51.19, 56.30, 136.97, 150,67	1.50, 1.47, 2.14, 2.72	NV
	R	102	0.87, 0.80	0.75, 0.63, 1.59, 1.86	47.91, 57.05, 136.97, 150.67	1.34, 1.09, 2.14. 2.72	NV
	$(B - R)$	102	0.80, 0.80	0.64, 0.64, 1.59, 1.86	57.75, 62.16, 136.97, 150.67	1.21, 1.62, 2. 14. 2.72	NV
17.08.09	B	56	0.85, 0.94	0.71, 0.88, 1.89, 2.34	67.24, 60.91, 82.29, 93.17	0.37, 1.03, 2.75, 3.78	NV
	R	56	0.95, 1.00	0.91, 0.99, 1.89, 2.34	41.80, 36.99, 82.29, 93.17	0.43, 1.14, 2. 75, 3.78	NV
	$(B - R)$	54	0.82, 0.81	0.67, 0.65, 1.91, 2.38	52.40, 58.65, 79.84, 90.57	0.24, 1.49, 2.76, 3.80	NV
20.08.09	B	44	0.98, 1.08	0.97, 1.16, 2.06, 2.63	34.34, 37.20, 67.46, 77.42	0.52, 0.52, 3.07, 4.36	NV
	R	49	0.98, 0.82	0.96, 0.68, 1.98, 2.49	30.25, 38.70, 73.68, 84.03	2.93, 2.73, 2.90, 4.05	NV
	$(B - R)$	44	1.52, 1.20	1.33, 1.44, 2.06, 2.63	36.38, 41.95, 67.46, 77.42	0.54, 0.67, 3.07, 4.36	NV
21.08.09	B	58	0.67, 0.75	0.45, 0.56, 1.87, 2.30	39.05, 36.87, 84.73, 95.75	1.09, 0.63, 2.75, 3.78	NV
	R	58	0.92, 0.87	0.85, 0.75, 1.87, 2.30	35.54, 39.42, 84.73, 95.75	1.47, 1.32, 2.75, 3.78	NV
	$(B - R)$	57	0.62, 0.82	0.39, 0.68, 1.88, 2.32	44.06, 28.95, 83.51, 94.46	0.92, 0.97, 2.75, 3.78	NV
27.08.09	B	90	1.23, 1.21	1.52, 1.47, 1.64, 1.94	62.78, 66.28, 122.94, 135.98	2.79, 2.69, 2.23, 2.86	NV
	R	90	1.08, 1.17	1.63, 1.36, 1.64, 1.94	81.52, 69.82, 122.94, 135.98	2.96, 2.49, 2.23, 2.8 6	NV
	$(B - R)$	90	1.15, 1.16	1.32, 1.34, 1.64, 1.94	74.46, 74.04, 122.94, 135.98	1.41, 1.64, 2.23, 2.8 6	NV
22.09.09	B	48	0.86, 0.81	0.75, 0.65, 1.99, 2.51	31.11, 37.60, 72.44, 82.72	3.81, 0.81, 3.05, 4.33	NV
	R	49	0.94, 0.75	0.88, 0.56, 1.98, 2.49	25.84, 43.25, 73.68, 84.03	1.81, 1.04, 3.05, 4.3 3	NV
	$(B - R)$	48	0.98, 0.83	0.96, 0.69, 1.99, 2.51	46.49, 65.99, 72.44, 82.72	0.77, 1.28, 3.05, 4.33	NV
03.10.09	B	60	0.88, 0.98	0.78, 0.96, 1.85, 2.27	35.08, 32.29, 87.17, 98.32	1.20, 1.03, 2.64, 3.58	NV
	R	60	1.01, 1.00	1.03, 1.00, 1.85, 2.27	42.00, 44.85, 87.17, 98.32	1.18, 2.16, 2.64, 3.58	NV
	$(B - R)$	60	0.99, 0.94	0.97, 0.89, 1.85, 2.27	35.12, 41.80, 87.17, 98.32	0.88, 0.66, 2.64, 3.5 8	NV
09.10.09	R	80	1.03, 0.97	1.06, 0.93, 1.70, 2.02	52.18, 56.23, 111.14, 123.59	2.17, 2.90, 2.33, 3.04	NV
09.05.10	R	96	1.42, 1.32	2.03, 1.74, 1.62, 1.90	41.08, 44.48, 129.97, 143.34	1.09, 0.66, 2.18, 2.79	NV
19.06.10	B	61	1.08, 1.08	1.18, 1.16, 1.84, 2.25	34.68, 34.60, 88.38, 99.61	0.66, 0.85, 2.64, 3.58	NV
	R	61	1.04, 1.07	1.07, 1.14, 1.84, 2.25	34.33, 30.73, 88.38, 99.61	0.86, 1.74, 2.64, 3.5 8	NV
	$(B - R)$	61	0.97, 0.93	0.95, 0.87, 1.84, 2.25	35.47, 35.16, 88.38, 98.61	0.53, 1.35, 2.64, 3.5 8	NV
15.07.10	B	20	0.76, 0.99	0.58, 0.99, 3.03, 4.47	23.79, 9.21, 36.19, 43.82	1.37, 0.44, 5.42, 9.34	NV
	R	18	1.04, 1.50	1.09, 0.25, 3.24, 4.92	3.51, 15.06, 33.41, 40.79	0.02, 0.17, 6.93, 12.97	NV
	$(B-R)$	19	0.85, 1.15	0.72, 1.32, 3.13, 4.68	28.38, 10.55, 34.81, 42.31	1.37, 0.44, 5.42, 9.34	NV
16.07.10	B	28	1.26, 1.27	1.58, 1.60, 2.51, 3.44	21.17, 15.18, 46.96, 55.48	0.33, 1.71, 3.99, 6.19	NV
	R	30	1.20, 1.19	1.43, 1.43, 2.42, 3.29	16.59, 16.66, 49.59, 58.30	1.45, 3.50, 3.90, 5.98	NV
	$(B - R)$	25	1.18, 1.18	1.39, 1.39, 2.66, 3.74	10.39, 07.40, 42.98, 51.18	0.24, 0.91, 4.43, 7.10	NV
17.07.10	R	80	1.06, 0.90	1.12, 0.80, 1.70, 2.02	57.98, 83.01, 111.14, 123.59	1.19, 0.82, 2.33, 3.04	NV
17.07.10	B	78	1.38, 1.04	1.91, 1.08, 1.71, 2.04	44.26, 52.82, 108.77, 121.10	2.16, 1.63, 2.39, 3.15	NV
	R	78	1.24, 1.17	1.55, 1.36, 1.71, 2.04	52.97, 43.59, 108.77, 121.10	1.49, 2.40, 2.39, 3.15	NV
	$(B - R)$	78	1.36, 1.14	1.84, 1.31, 1.71, 2.04	74.62, 76.24, 108.77, 121.10	3.28, 2.73, 2.39, 3.15	NV

Table 5 – *continued*

Date	Band	N	C-test C_1, C_2	F-test $F_1, F_2, F_c(0.99), F_c(0.999)$	χ^2 test $\chi^2_1, \chi^2_2, \chi^2_{0.99}, \chi^2_{0.999}$	ANOVA $F_1, F_2, F_c(0.99), F_c(0.999)$	Variable
19.07.10	B	62	1.18, 0.90	1.40, 0.81, 1.83, 2.24	28.47, 35.09, 89.59, 100.89	4.06, 1.93, 2.64, 3.58	NV
	R	62	1.02, 1.02	1.03, 1.05, 1.83, 2.24	34.71, 24.71, 89.59, 100.89	0.82, 1.92, 2.64, 3.58	NV
	$(B-R)$	62	1.14, 0.95	1.31, 0.91, 1.83, 2.24	43.18, 43.04, 89.59, 100.89	2.23, 1.51, 2.64, 3.58	NV
21.07.10	B	72	1.16, 1.05	1.35, 1.09, 1.75, 2.11	43.77, 37.64, 101.62, 113.58	1.49, 0.77, 2.47, 3.27	NV
	R	72	1.29, 1.08	1.65, 1.16, 1.75, 2.11	49.95, 51.39, 101.62, 113.58	1.80, 1.44, 2.47, 3.27	NV
	$(B-R)$	72	1.20, 1.05	1.45, 1.10, 1.75, 2.11	57.21, 50.85, 101.62, 113.58	1.58, 0.93, 2.47, 3.27	NV
05.08.10	B	19	2.31, 2.05	5.34, 4.19, 3.13, 4.68	130.68, 85.15, 34.81, 42.31	5.00, 12.38, 5.42, 9.34	NV
	R	20	1.91, 1.96	3.64, 3.84, 3.03, 4.47	19.83, 14.16, 36.19, 43.82	2.90, 4.54, 5.29, 9.01	NV
	$(B-R)$	20	2.15, 1.83	4.64, 3.36, 3.03, 4.47	96.74, 69.81, 36.19, 43.82	4.95, 11.4, 5.29, 9.01	NV
10.08.10	B	12	1.38, 0.99	1.91, 0.98, 4.46, 7.76	14.21, 16.80, 24.72, 31.26	0.001, 0.02, 11.26, 25.41	NV
	R	14	1.34, 0.94	1.80, 0.89, 3.91, 6.41	5.70, 10.91, 27.69, 34.53	0.20, 0.68, 7.21, 13.81	NV
	$(B-R)$	14	1.43, 1.17	2.05, 1.36, 3.91, 6.41	21.69, 27.11, 27.69, 34.53	0.29, 0.18, 7.21, 13.81	NV

V: variable, NV: non-variable.

significance with respect to star 1 they never do so with respect to star 2. Hence, this source was also very stable during each individual night of the observation period. The differential light curves of 1ES 2344+514 are given in Figs 3 and 4 for these 14 nights.

4.3 Results for short-term variability

We quantify our results of STV using two statistics: *C*- and *F*-tests (Table 7). This is because in an ANOVA test we must compare the means of a number of similar samples or groups of measurements which is not possible for our short-term observations. Also, χ^2 test compares the variation of an object with its photometric errors. Moreover, the errors from DAOPHOT are usually underestimated because of which we need to introduce a correction factor by which these errors are multiplied. This factor comes from a comparison between the variation and the errors of two intrinsically non-variable stars. As mentioned below, for our source 1ES 2344+514, two or perhaps more than two out of three standard stars present in the field are slowly varying. So, in this case, the correction factor is underestimated and not just typically 1.3–1.75 and the χ^2 test is not applicable here. Hence, we are not using ANOVA and χ^2 test in STV analysis.

4.3.1 1ES 1959+650

We have examined the source 1ES 1959+650 for STV during 44 nights (in *B*, *V*, *R* and *I* bands) between 2009 July and 2010 November (Fig. 5).

B passband: the short-term light curve of 1ES 1959+650 in the *B* band is displayed in the upper panel of Fig. 5. The maximum variation noticed in the light curve of the source is 1.23 mag (between its brightest level at 14.99 mag on JD 245 5036.402 07 and the faintest level at 16.22 mag on JD 245 5330.405 54). The values of *C*- and *F*-tests support the existence of short-term variation of the source in the *B*-band observations. We calculated the STV amplitude using equation (3) and found that source has varied ≈102 per cent.

V passband: the *V*-band short-term light curve of 1ES 1959+650 is shown in the second panel of Fig. 5. The maximum variation seen is 1.06 mag (between its brightest level at 14.429 on JD 245 5036.408 11 and the faintest level at 15.490 on JD 245 5330.403 01). The *C*- and *F*-tests again support the existence of short-term variation of the source in the *V*-band observations. We

calculated that this source has a variability amplitude of ≈90 per cent.

R passband: the third panel of Fig. 5 gives the *R* band short-term light curve of 1ES 1959+650. The maximum variation noticed in the source is 0.94 mag (between its brightest level at 14.015 on JD 245 5041.327 82 and the faintest level at 14.959 on JD 245 5326.415 14). The values of the *C*- and *F*-test calculations also support the existence of STV in our source. The amplitude of variability in the source is ≈82 per cent.

I passband: the short-term light curve of 1ES 1959+650 in the *I* band is displayed in the fourth panel of Fig. 5. The maximum variation noticed in the source is 0.85 mag (between its brightest level at 13.49 mag on JD 245 5036.400 52 and the faintest level at 14.34 mag on JD 245 5330.393 05). Again, the *C*- and *F*-tests both support the existence of short-term variations of the source in these *I*-band observations. The amplitude of variability in the source is ≈75 per cent.

(V − R) colour: the $(V - R)$ colour index of 1ES 1959+650 in the $(V - R)$ over this period comprises the bottom panel of Fig. 5. The maximum variation we saw in the source is 0.39 (between its colour index of 0.29 on JD 245 5395.382 34 and 0.68 at JD 245 5161.261 57). Both the *C*- and *F*-tests show significant $(V - R)$ colour variations in our observations. The amplitude of variability in the source's colour is ≈36 per cent.

4.3.2 1ES 2344+514

We have examined the source 1ES 2344+514 on 39 nights (in *B*, *V*, *R* and *I* bands) ranging from 2009 August to 2010 November for STV (shown in Fig. 6). Because of the variation in the standard stars present in the field of this blazar, we noticed variations in 1ES 2344+514 in each band. Perhaps two out of three standard stars have slow variations which are propagating in the source. Therefore, despite the nominally large variation in the blazar calibrated magnitude, neither the *C*-test nor the *F*-test supports the existence of short-term variation of the source in 1ES 2344+514. Also, similar behaviours of standard stars were noticed in Tuorla Observatory observations.[3]

The maximum variation noticed in the short-term differential *B*-band light curve of 1ES 2344+514 is 0.80 mag (between
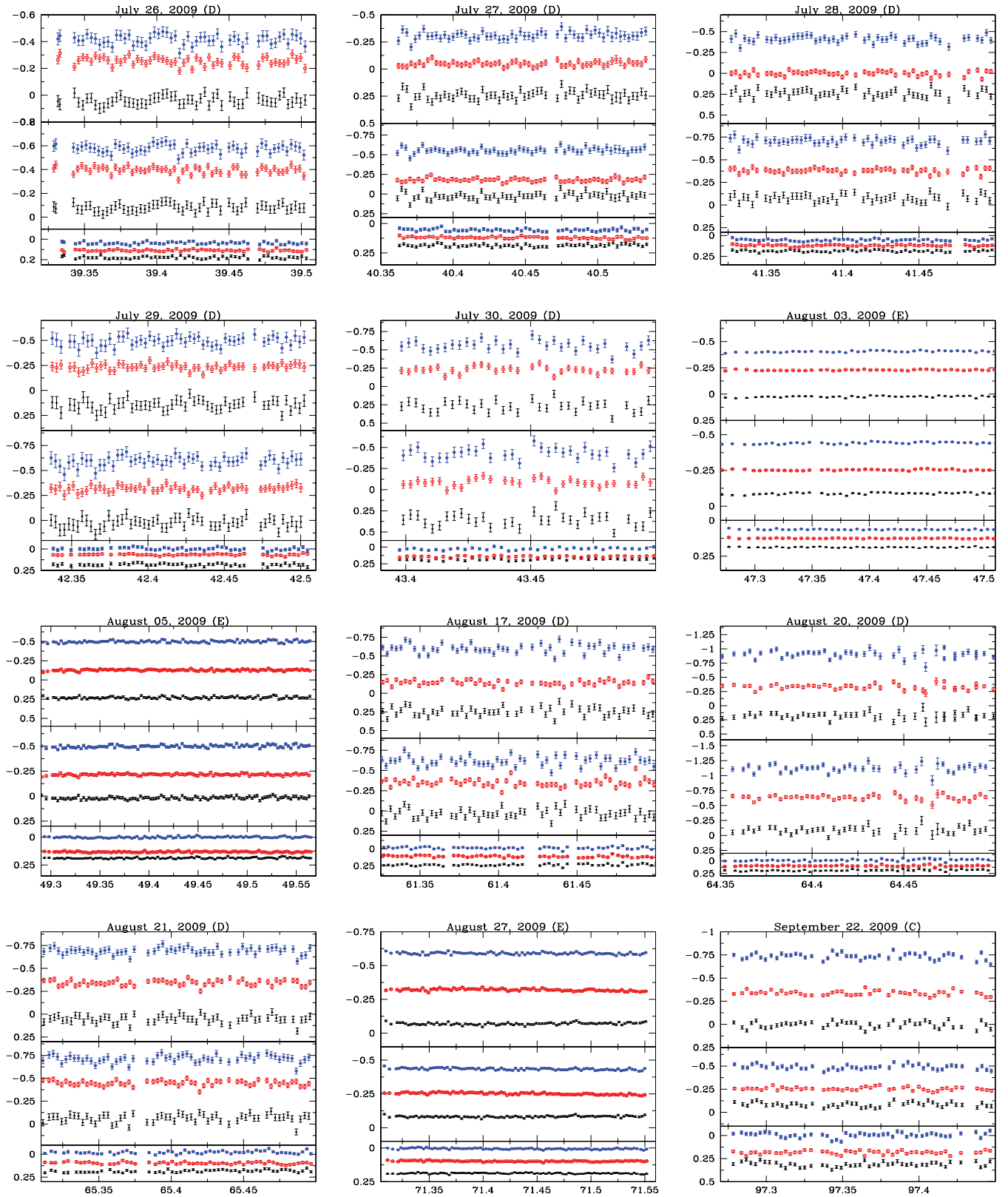
[3] http://users.utu.fi/kani/1m/

Figure 1. The *B* (middle panel), *R* (lower panel) and (*B* − *R*) (upper panel) light curves of 1ES 1959+650. The *x*-axis is JD (245 5000+) and the *y*-axis is the differential instrumental magnitude. Open circles (also in red colour) show the differential light curve (DLC) of blazar–star 1, filled circles (in blue colour) show the DLC of blazar–star 2 while star symbols (in black colour) represent DLC of comparison stars (star 1–star 2). Dates and telescopes are given on top of each plot. The magnitudes of each band are adjusted with an arbitrary offset (for clarity) in each panel of figure.
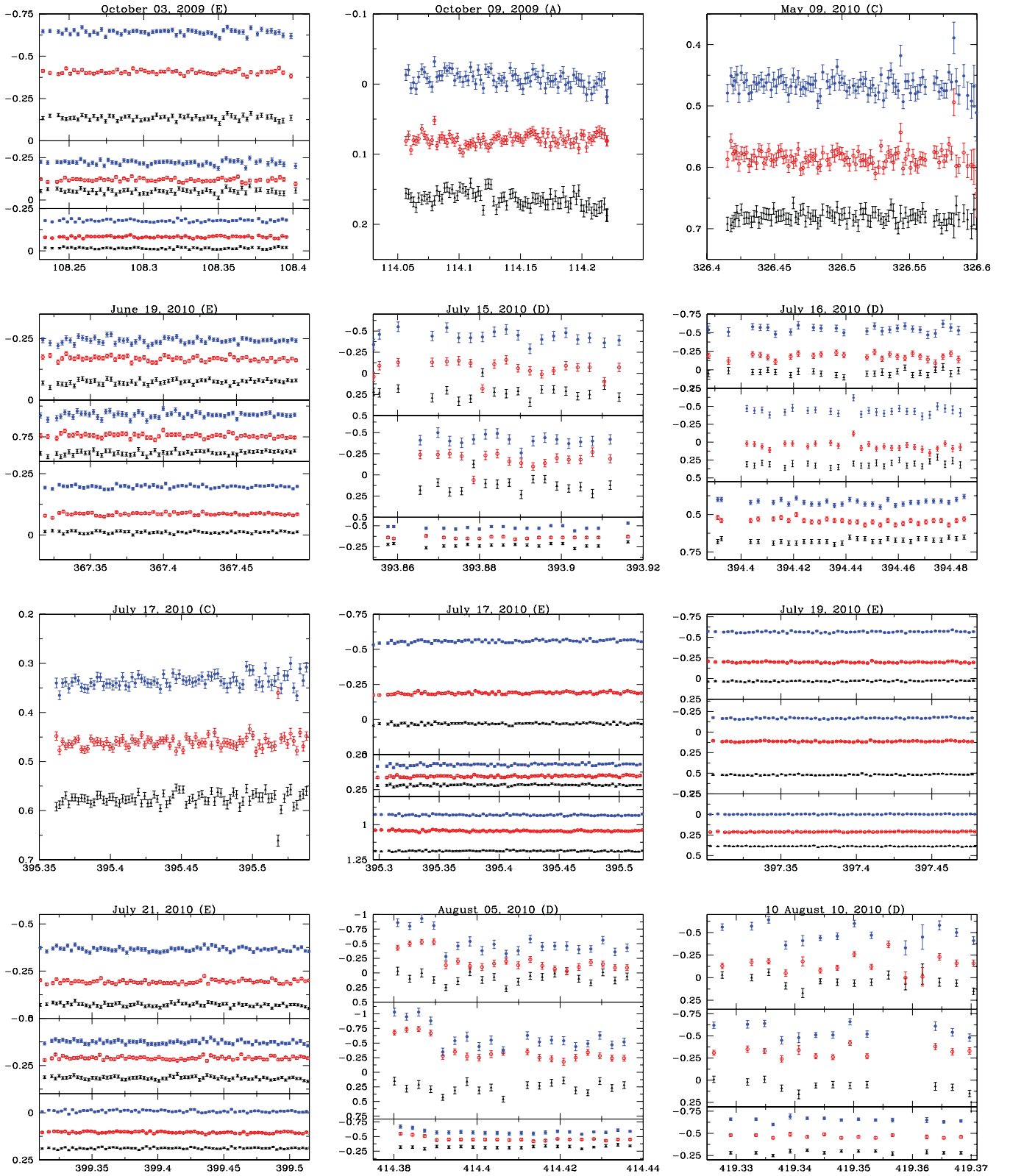
Figure 2. As in Fig. 1 for additional nights for 1ES 1959+650.

its brightest level at 2.02 mag on JD 245 5065.481 44 and the faintest level at 1.22 mag on JD 245 5449.577 56) and the variation in the differential instrumental magnitudes of standard stars is 0.53. Because the stellar differential magnitudes varied so

much, none of them could be truly considered to be of fixed brightness.

The maximum variation we found in the short-term light curve of this source in *V* band is 0.73 mag (between its brightest

Table 6. Results of intraday variability observations of 1ES 2344+514.

Date	Band	N	C-test C_1, C_2	F-test $F_1, F_2, F_c(0.99), F_c(0.999)$	χ^2 test $\chi_1^2, \chi_2^2, \chi_{0.99}^2, \chi_{0.999}^2$	ANOVA $F_1, F_2, F_c(0.99), F_c(0.999)$	Variable
04.08.09	B	52	1.03, 1.61	1.05, 2.60, 1.94, 2.42	33.86, 32.56, 77.39, 87.97	3.88, 2.89, 2.89, 4.02	NV
	R	52	1.06, 1.27	1.11, 1.60, 1.94, 2.42	58.70, 93.56, 77.39, 87.97	3.17, 0.95, 2.89, 4.02	NV
	$(B-R)$	52	0.79, 1.43	0.63, 2.06, 1.94, 2.42	65.52, 49.98, 77.39, 87.97	2.54, 2.24, 2.89, 4.02	NV
18.08.09	B	40	1.02, 1.19	1.04, 1.43, 2.14, 2.76	29.53, 42.65, 62.43, 72.05	1.38, 0.54, 3.26, 4.72	NV
	R	39	1.02, 1.13	1.03, 1.27, 2.16, 2.80	28.04, 53.42, 61.16, 70.70	1.12, 0.99, 3.28, 4.77	NV
	$(B-R)$	40	0.95, 1.14	0.91, 1.30, 2.14, 2.76	25.29, 34.61, 62.43, 72.05	1.11, 0.29, 3.26, 4.72	NV
19.08.09	B	40	1.26, 1.54	1.59, 2.37, 2.14, 2.76	42.25, 57.83, 62.43, 72.05	0.79, 0.66, 3.26, 4.72	NV
	R	35	0.88, 1.13	0.77, 1.27, 2.16, 2.80	21.39, 23.44, 61.16, 70.70	4.47, 1.86, 3.52, 5.24	NV
	$(B-R)$	38	1.49, 1.60	2.21, 2.55, 2.18, 2.84	42.29, 68.94, 59.89, 69.35	0.63, 0.52, 3.30, 4.82	NV
22.08.09	B	36	0.89, 1.22	0.79, 1.26, 2.23, 2.93	3.30, 4.02, 57.34, 66.62	1.35, 1.03, 3.53, 5.24	NV
	R	36	1.00, 1.14	0.99, 1.30, 2.23, 2.93	5.71, 9.47, 57.34, 66.62	8.38, 1.22, 3.53, 5.24	NV
	$(B-R)$	36	0.91, 1.31	0.83, 1.72, 2.23, 2.93	4.13, 4.02, 57.34, 66.62	1.68, 1.14, 3.53, 5.24	NV
25.08.09	B	42	0.79, 1.14	0.63, 1.29, 2.09, 2.69	33.59, 40.27, 64.95, 74.74	1.34, 0.91, 3.26, 4.72	NV
	R	41	0.81, 1.13	0.65, 1.28, 2.11, 2.73	31.64, 34.89, 63.69, 73.40	3.29, 3.01, 3.26, 4.72	NV
	$(B-R)$	40	0.90, 1.17	0.81, 1.38, 2.14, 2.76	30.94, 38.88, 62.43, 72.05	0.93, 1.61, 3.26, 4.72	NV
26.08.09	B	45	0.70, 1.28	0.49, 1.64, 2.04, 2.60	45.26, 27.02, 68.71, 78.75	2.57, 2.98, 3.05, 4.33	NV
	R	44	0.79, 1.21	0.62, 1.47, 2.06, 2.63	44.04, 39.80, 67.46, 77.42	3.19, 1.41, 3.07, 4.36	NV
	$(B-R)$	43	0.74, 1.28	0.54, 1.63, 2.08, 2.66	47.39, 32.06, 66.21, 76.08	2.25, 2.51, 3.09, 4.40	NV
28.08.09	B	41	0.91, 1.08	0.82, 1.67, 2.11, 2.73	30.99, 47.19, 63.69, 73.40	2.89, 0.45, 3.26, 5.72	NV
	R	42	0.79, 1.31	0.62, 1.73, 2.09, 2.69	58.94, 48.06, 64.95, 74.74	2.08, 1.27, 3.26, 4.72	NV
	$(B-R)$	40	0.84, 1.19	0.70, 1.43, 2.14, 2.76	45.68, 51.62, 63.69, 73.40	1.10, 0.21, 3.26, 4.72	NV
29.08.09	B	54	1.19, 1.08	1.41, 1.67, 1.91, 2.38	65.84, 184,10, 70.84, 90.57	23.90, 5.31, 2.76, 3.80	NV
	R	54	0.96, 0.53	0.87, 0.28, 1.91, 2.38	23.77, 168.72, 70.84, 90.57	45.68, 0.46, 2.78, 3.80	NV
	$(B-R)$	54	0.82, 1.37	0.67, 1.86, 1.92, 2.40	74.12, 63.93, 78.62, 89.27	4.31, 6.01, 2.78, 3.82	NV
18.09.09	B	41	0.84, 1.03	0.71, 1.05, 2.11, 2.73	18.36, 26.20, 63.69, 73.40	1.86, 0.44, 3.26, 4.72	NV
	R	41	0.77, 1.24	0.60, 1.55, 2.11, 2.73	40.81, 30.21, 63.69, 73.40	2.51, 2.65, 3.26, 4.72	NV
	$(B-R)$	41	0.85, 1.17	0.72, 1.37, 2.11, 2.73	28.46, 33.43, 63.69, 73.40	2.11, 0.59, 3.26, 4.72	NV
21.09.09	B	32	1.35, 1.74	1.83, 3.03, 2.35, 3.15	26.68, 36.38, 52.19, 61.10	4.93, 2.99, 3.90, 5.98	NV
	R	29	0.79, 1.12	0.63, 1.25, 2.46, 3.36	17.05, 21.27, 48.29, 56.89	1.07, 0.13, 3.94, 6.08	NV
	$(B-R)$	24	0.89, 1.05	0.80, 1.11, 2.72, 3.85	21.50, 35.26, 41.64, 49.73	0.93, 0.37, 4.50, 7.27	NV
03.10.09	B	24	0.81, 1.34	0.65, 1.80, 2.72, 3.85	13.61, 10.86, 41.64, 49.73	0.17, 0.12, 4.50, 7.27	NV
	R	26	1.04, 1.49	1.09, 2.22, 2.60, 3.63	24.47, 31.23, 44.31, 52.62	3.06, 2.20, 4.43, 7.10	NV
	$(B-R)$	25	0.85, 1.35	0.72, 1.83, 2.66, 3.74	15.18, 13.49, 42.98, 51.18	0.31, 0.40, 4.43, 7.10	NV
10.10.09	R	65	0.95, 0.14	0.90, 0.02, 1.80, 2.19	33.84, 62.33, 93.22, 104.72	4.27, 2.73, 2.55, 3.41	NV
10.01.10	R	49	1.45, 1.63	2.06, 2.66, 1.98, 2.49	31.55, 56.13, 73.68, 84.04	6.71, 6.99, 2.90, 4.05	NV
11.01.10	R	50	0.68, 0.82	0.46, 0.67, 1.96, 2.46	17.32, 26.85, 74.92, 85.35	2.41, 1.07, 2.89, 4.02	NV
20.01.10	R	30	0.88, 1.10	0.77, 1.22, 2.42, 3.29	12.68, 19.40, 49.59, 58.30	3.47, 0.70, 3.90, 5.98	NV
18.07.10	R	115	0.84, 1.14	0.72, 1.31, 1.55, 1.79	63.09, 67.71, 152.04, 166.41	0.78, 1.11, 2.04, 2.55	NV
18.07.10	B	62	0.85, 1.20	0.72, 1.45, 1.83, 2.24	31.49, 36.59, 89.59, 100.89	0.45, 1.89, 2.64, 3.58	NV
	R	62	1.06, 1.39	1.13, 1.92, 1.83, 2.24	60.00, 67.95, 89.59, 100.89	4.09, 3.75, 2.64, 3.58	NV
	$(B-R)$	62	0.82, 1.19	0.67, 1.41, 1.83, 2.24	42.62, 42.68, 89.59, 100.89	0.87, 1.92, 2.64, 3.59	NV
20.07.10	B	86	0.69, 1.20	0.47, 1.43, 1.66, 1.97	56.45, 50.61, 118.24, 131.04	0.87, 1.05, 2.28, 2.95	NV
	R	86	0.93, 1.12	0.86, 1.25, 1.66, 1.97	55.47, 99.15, 118.24, 131.04	1.36, 1.00, 2.28, 2.95	NV
	$(B-R)$	86	0.77, 1.23	0.59, 1.52, 1.66, 1.97	63.49, 75.00, 118.24, 131.04	0.69, 0.70, 2.28, 2.95	NV
22.07.10	B	16	0.83, 1.12	0.68, 1.25, 3.52, 5.54	3.22, 4.71, 30.58, 37.70	1.28, 0.37, 6.93, 12.97	NV
	R	17	0.71, 0.78	0.51, 0.61, 3.37, 5.20	4.44, 8.51, 32.00, 39.25	0.27, 4.04, 6.93, 12.97	NV
	$(B-R)$	16	0.69, 1.05	0.48, 1.10, 3.52, 5.54	3.40, 3.72, 30.58, 37.70	2.12, 1.90, 6.93, 12.97	NV

V: variable, NV: non-variable.

level at 15.47 mag on JD 245 5449.572 30 and the faintest level at 16.20 mag on JD 245 5065.478 06). The variation in the differential instrumental magnitudes of standard stars is 0.45.

The *R*-band maximum variation we found was 0.65 mag (between its brightest level at 14.72 mag on JD 245 5449.561 90 and the faintest level at 15.37 mag on JD 245 5070.411 22). The varia-

tion in the differential instrumental magnitudes of standard stars is 0.44.

The maximum variation noticed in the light curve of the source in *I* band is 0.62 mag (between its brightest level at 13.92 mag on JD 245 5449.557 30 and the faintest level at 14.52 mag on JD 245 5063.503 16). The variation in the differential instrumental magnitudes of standard stars is 0.55.
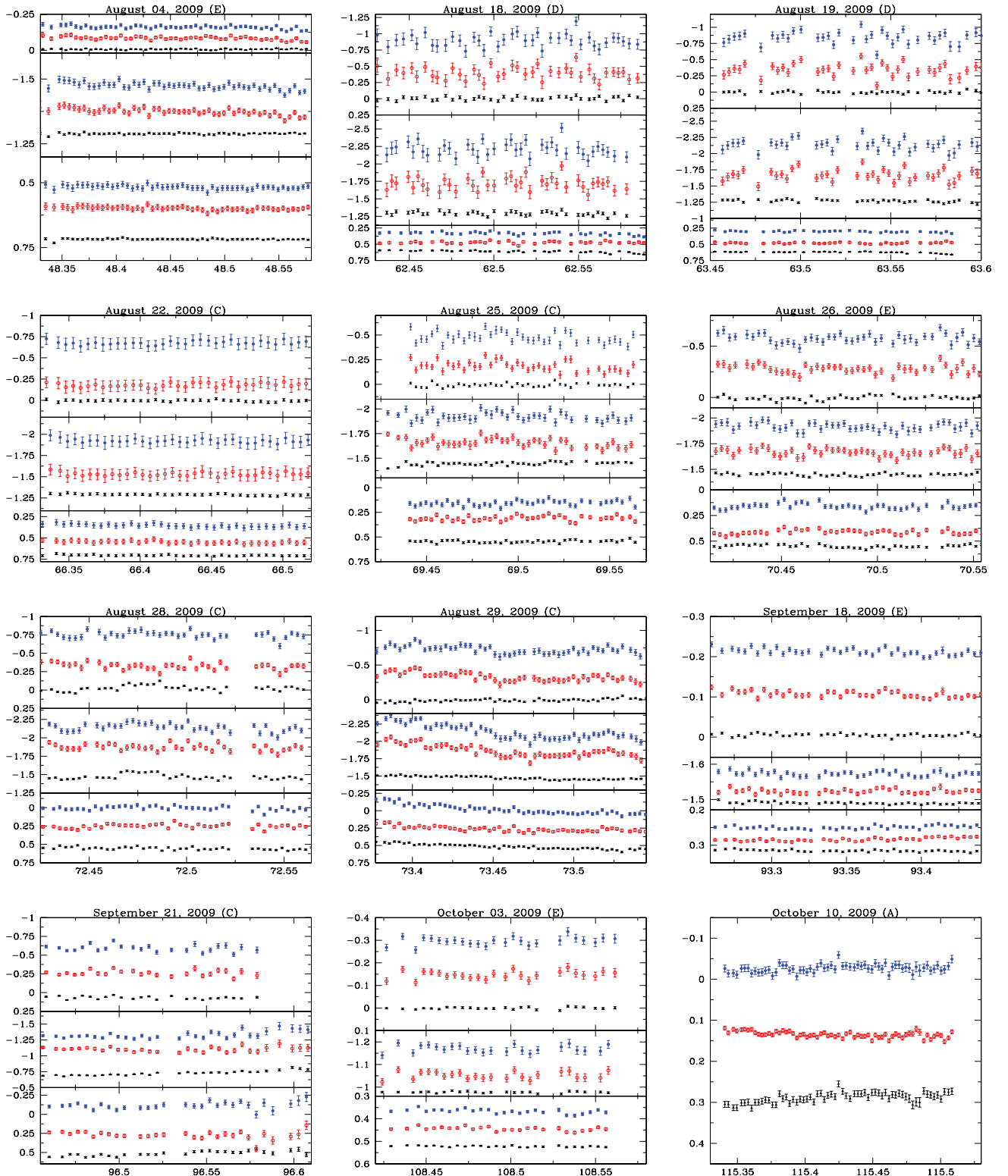
Figure 3. As in Fig. 1 for 1ES 2344+514.

Finally, the maximum difference in the $(V - R)$ colour for 1ES 2344+514 is 0.22 mag (between its colour range 0.62 mag on JD 245 5070.410 47 and 0.84 mag at JD 245 5065.476 56). The variation in the differential instrumental magnitudes of standard stars is 0.16.

5 DISCUSSION AND CONCLUSION

We have presented our results of quasi-simultaneous and relatively dense temporal observations of two HBLs, 1ES 1959+650 and 1ES 2344+514, in two optical bands (B and R) during 2009–2010. These are the first extensive observations of this type of these two blazars
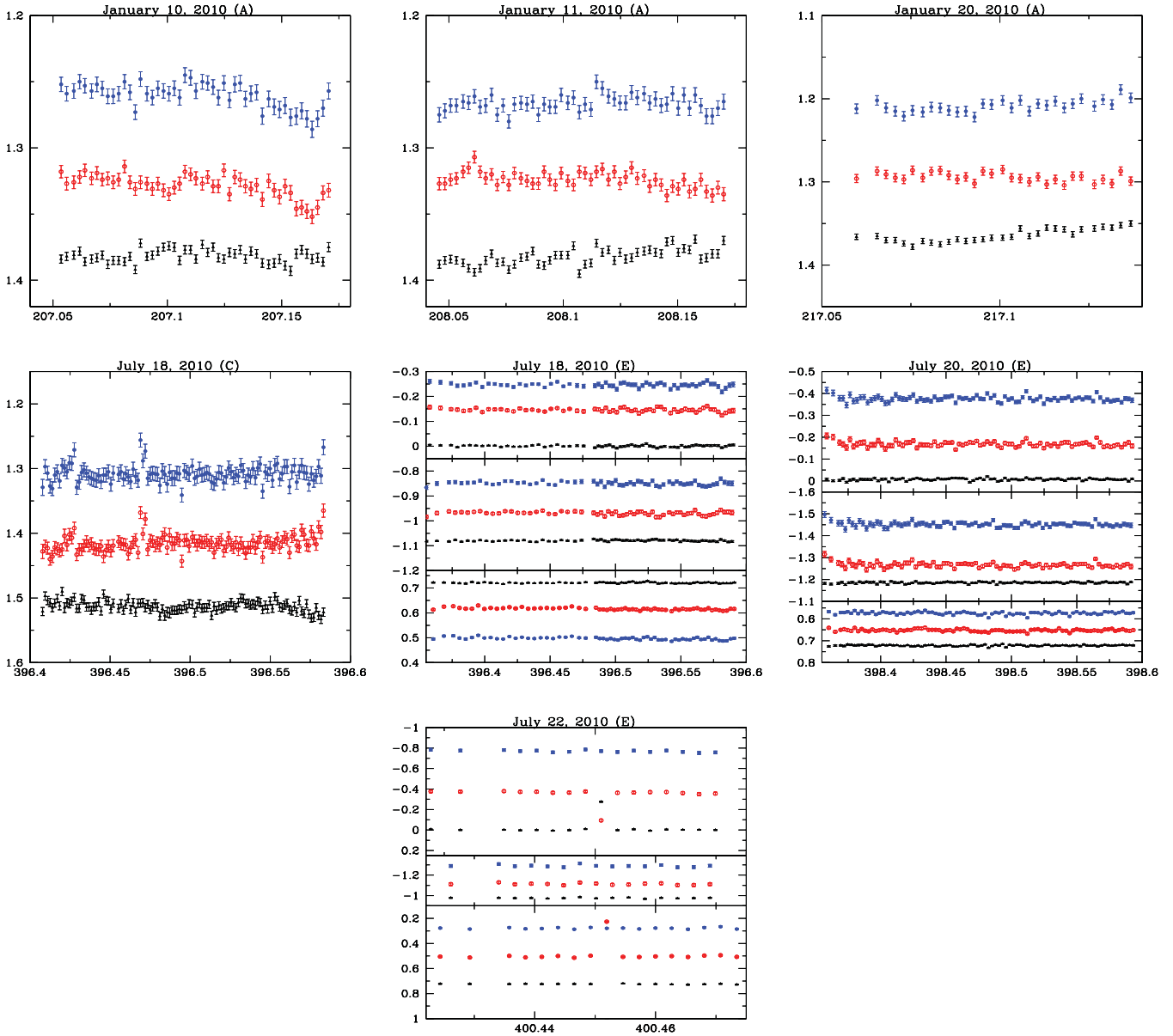
Figure 4. As in Fig. 1 for 1 ES 2344+514.

Table 7. Results of short-term variability observations.

Source name	Band	N	C-test C_1, C_2	F $F_1, F_2, F_c(0.99), F_c(0.999)$	Variable	A (per cent)
1ES 1959+650	B	75	4.25, 4.21	18.05, 17.69, 1.73, 2.07	V	102.4
	V	75	5.48, 5.65	29.99, 31.91, 1.73, 2.07	V	90.4
	R	81	11.87, 11.83	140.80, 139.89, 1.69, 2.01	V	81.5
	I	78	9.09, 9.14	82.59, 83.49, 1.71, 2.04	V	74.5
	$(V - R)$	75	3.26, 2.84	10.64, 8.09, 1.73, 2.07	V	36.0
1ES 2344+514	B	39	1.50, 0.61	2.24, 0.37, 2.16, 2.80	NV	–
	V	39	1.95, 1.54	3.78, 2.38, 2.16, 2.80	NV	–
	R	38	1.94, 1.37	3.77, 1.88, 2.18, 2.84	NV	–
	I	39	1.72, 1.39	2.97, 1.94, 2.16, 2.80	NV	–
	$(V - R)$	38	1.08, 0.83	1.17, 0.69, 2.18, 2.84	NV	–

V: variable, NV: non-variable.
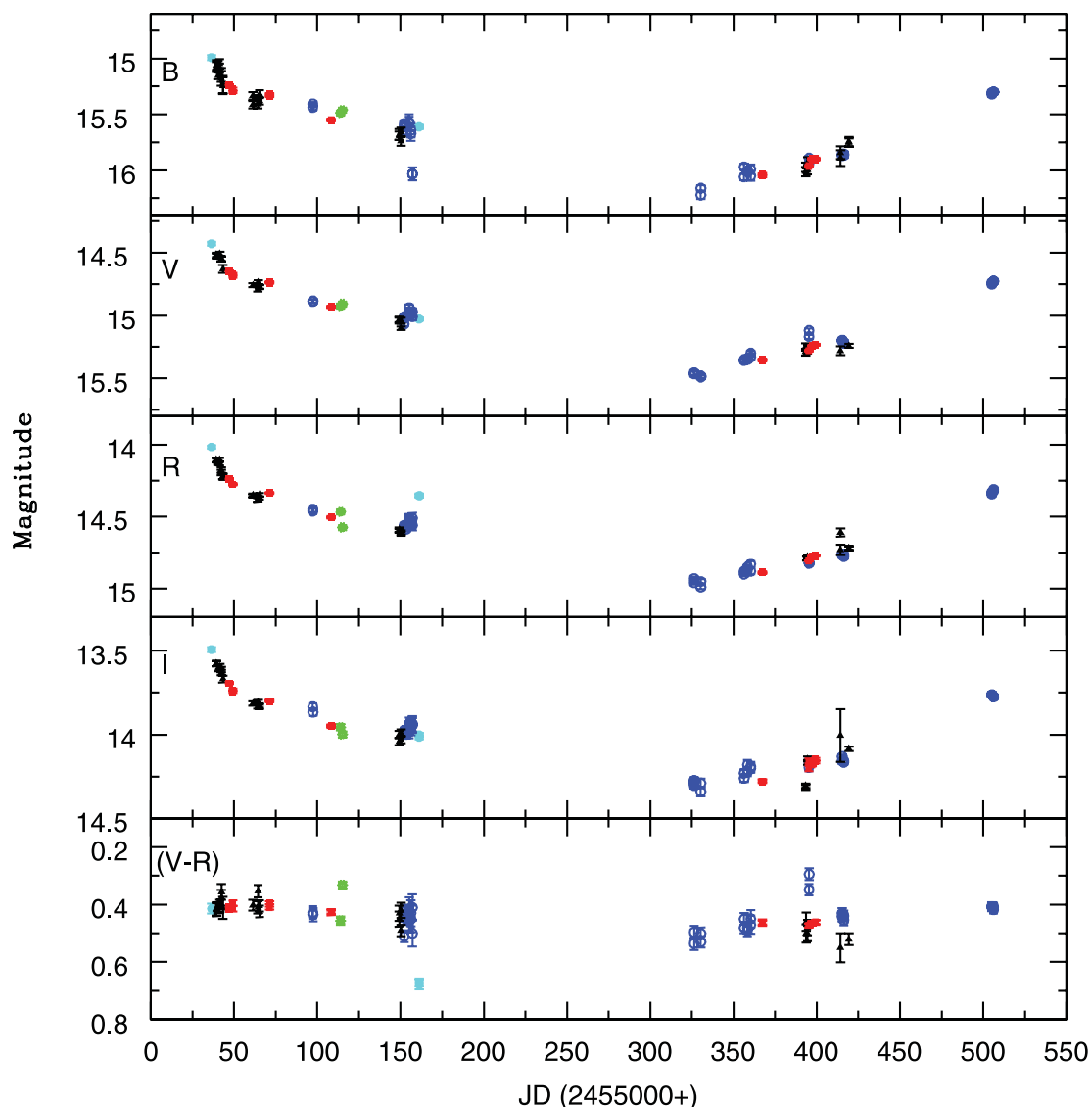
Figure 5. Short-term variability light curve of 1ES 1959+650. Starred, solid circle, open circle, triangle and square symbols represent data from the telescopes A, B, C, D and E, respectively.

and thus adds to the rather small amount of data on HBL microvariability and STV. We have observed the sources 1ES 1959+650 and 1ES 2344+514 on 24 and 19 nights, respectively, but no significant IDV was observed during any night for those two targets. In addition, we can report the results of STV studies of these sources. The blazar 1ES 1959+650 has shown genuine STV and it can be characterized by a preliminary fading trend of ∼0.6 mag (from JD 245 5036 to 245 5161) and then a brightening trend of ∼0.74 (from JD 245 5326 to 245 5506 in *V* band). However, despite nominally substantial magnitude changes, genuine STV was not found for the source 1ES 2344+514. We found that most of the apparent variations by the blazar could have arisen from slow variations in the 'standard' stars in the field. The results presented here make an important contribution to the study of these target objects, as such extensive studies have not yet been performed on their intranight time-scales and the optical behaviour of this class of BL Lacs is still largely unknown. Our measurements provide quasi-simultaneous measurements in two bands, unlike most earlier microvariability studies.

There are several theoretical models that might be able to explain the observed variability over wide time-scales for all bands, with the leading contenders based upon shocks propagating down relativistic jets (e.g. Marscher & Gear 1985; Hughes, Aller & Aller 1991; Qian et al. 1991; Marscher, Gear & Travis 1992; Wagner & Witzel 1995; Marscher 1996). In this class of models much of the variability arises when a shock strikes a feature in the jet. Some of the variability may arise from helical structures, precession or other geometrical effects occurring within the jets (e.g. Camenzind & Krockenberger 1992; Gopal-Krishna & Wiita 1992). These models seem to provide reasonable, albeit generic, representations of the variations observed on time-scales from about a day up through months and probably, years. Hotspots or disturbances in or above accretion discs surrounding the BHs at the centres of AGNs (e.g. Chakrabarti & Wiita 1993; Mangalam & Wiita 1993) are likely to play a key role in the variability of non-blazar AGNs and might provide seed fluctuations that could be advected into the blazar jet and then Doppler amplified in the relativistic jets.
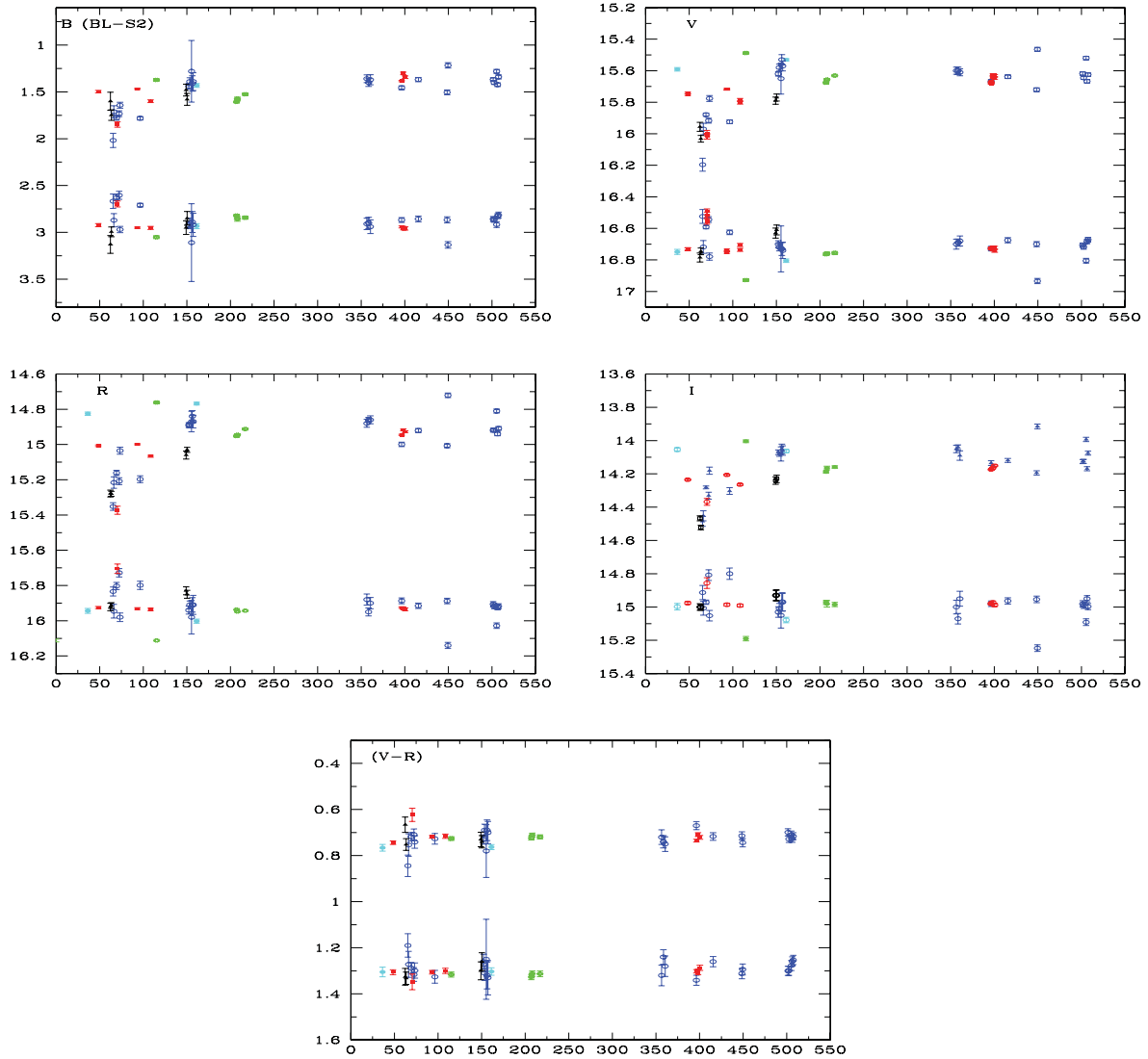
Figure 6. Short-term variability light curve of 1ES 2344+514. Starred, solid circle, open circle, triangle and square symbols represent data from the telescopes A, B, C, D and E, respectively. *y*-axis is magnitude and *x*-axis is JD (245 5000+) in each plot. In the *B*-band data set, the upper LC is (blazar–star1) and the lower one is the differential magnitude of (star1–star2). In the remaining panels, the upper curves are the calibrated blazar magnitudes and lower ones are differential magnitudes of (star1–star2) in V, R, I and $(V - R)$.

Previous observational results have indicated that HBLs show a statistically significantly lesser amount of optical variability than the LBLs do (Stocke et al. 1985, Stocke et al. 1989; Heidt & Wagner 1996), and this conclusion is supported by our results, in that neither of these two HBLs ever showed microvariability. Sambruna, Maraschi & Urry (1996) investigated the multifrequency spectral properties of LBLs and HBLs and mentioned that these spectral properties require a systematic change of intrinsic physical parameters, such as magnetic field, jet size and maximum electron energy, and this change is in the sense that HBLs have higher magnetic fields/electron energies and smaller sizes than LBLs. The difference in the IDV behaviour of HBLs could be due to the effect of stronger magnetic fields and/or electron energies in these objects (Sambruna et al. 1996) that could prevent or delay the formation of features like density inhomogeneities and bends in the bases of the jets by Kelvin–Helmholtz instabilities (Romero et al. 1999). For instance, in the model proposed by Sol, Pelletier & Asseo (1989),

extragalactic jets are composed of two different fluids, a highly relativistic spine and a slower sheath. Kelvin–Helmholtz instabilities must arise at the interface between these two fluids with different bulk velocities. Such instabilities might be responsible for many of the knots and bends observed in the large-scale structures of jets. Romero (1995) showed that axial magnetic fields prevent the development of Kelvin–Helmholtz instabilities in sub-parsec to parsec scale jets if their values exceed the critical value B_c given by

$$B_c = [4\pi n m_e c^2 (\gamma^2 - 1)]^{1/2} \gamma^{-1}, \tag{5}$$

where n is the local electron density, m_e is the electron rest mass and γ is the central flow's bulk Lorentz factor. So, if $B > B_c$ this class of instabilities will be suppressed. However, if $B < B_c$ the Kelvin–Helmholtz instabilities can produce significant changes in the jet morphology, and these features could be responsible for rapid variability when the relativistic shock waves interact with them. So if HBLs typically possess stronger magnetic fields for given electron

densities or lower electron densities for given field strengths, then we suggest that such a reduction in Kelvin–Helmholtz instabilities would reduce the incidence of microvariability in the optical light curves.

Another possible explanation for the difference between the optical variability behaviour of the LBL and HBL classes of blazars can dispense with the hypothesis of suppressed Kelvin–Helmholtz instabilities. We recall that the optical band is near or above the peak of the first hump in the SED for LBLs but below that peak for HBLs. Therefore changes in the efficiency of acceleration of, and/or in the rates at which energy is radiated by, the highest energy electrons available for synchrotron emission would have a large and rapid effect on the emitted flux in those bands for LBLs. However, those variations would have a more modest and more retarded effect on optical variability in HBLs, since their optical emission is below the peak of the synchrotron emission. Such variations in acceleration efficiency could arise from changes in the local number density of the most energetic electrons or the strengths of the maximum localized magnetic fields. While magnetohydrodynamic instabilities might be the origin of such variations, so might the presence of turbulence in the vicinity of the shock (e.g. Marscher et al. 1992). If this is the case, then X-ray variability should be more pronounced for HBLs than for LBLs, in that the peak of the synchrotron emission lies near the X-ray band for the former class.

ACKNOWLEDGMENTS

REFERENCES

Abdo A. A. et al., 2010, ApJ, 715, 429
Aharonian F. et al., 2003, A&A, 406, L9
Albert J. et al., 2006, ApJ, 639, 761
Albert J. et al., 2007, ApJ, 662, 892
Bachev R., Strigachev A., Semkov E., 2005, MNRAS, 358, 774
Beckmann V., Wolter A., Celotti A., Costamante L., Ghisellini G., Maccacaro T., Tagliaferri G., 2002, A&A, 383, 410
Böttcher M., 2005, ApJ, 621, 176
Camenzind M., Krockenberger M., 1992, A&A, 255, 59
Carini M. T., Miller H. R., 1992, ApJ, 385, 146
Catanese M. et al., 1998, ApJ, 501, 616
Chakrabarti S. K., Wiita P. J., 1993, ApJ, 411, 602
Dai B. Z., Xie G. Z., Li K. H., Zhou S. B., Liu W. W., Jiang Z. J., 2001, AJ, 122, 2901
Daniel M. K. et al., 2005, ApJ, 621, 181
de Diego J. A., 2010, AJ, 139, 1269
de Diego J. A., Dultzin-Hacyan D., Ramírez A., Benitez E., 1998, ApJ, 501, 69
Doroshenko V. T., Sergeev S. G., Efimov Y. S., Nazarov S., Pronik V. I., Sergeeva E. A., Sivtsov G. A., 2007, Astrophysics, 50, 40
Elvis M., Plummer D., Schachter J., Fabbiano G., 1992, ApJS, 80, 257
Falomo R., Kotilainen J. K., Treves A., 2002, ApJ, 569, L35
Fan J.-H., Kurtanidze O. M., Nikolashvili M. G., Gupta A. C., Zhang J.-S., Yuan Y.-H., 2004, Chinese J. Astron. Astrophys., 4, 133
Fiorucci M., Tosti G., Rizzi N., 1998, PASP, 110, 105
Fossati G., Maraschi L., Celotti A., Comastri A., Ghisellini G., 1998, MNRAS, 299, 433

Ghisellini G. et al., 1997, A&A, 327, 61
Ghisellini G., Celotti A., Fossati G., Maraschi L., Comastri A., 1998, MNRAS, 301, 451
Giommi P., Ansari S. G., Micol A., 1995, A&AS, 109, 267
Giommi P., Padovani P., Perlman E., 2000, MNRAS, 317, 743
Gopal-Krishna, Wiita P. J., 1992, A&A, 259, 109
Gopal-Krishna, Stalin C. S., Sagar R., Wiita P. J., 2003, ApJ, 586, L25
Grube J., 2008, in Aharonian F. A., Hofmann W., Rieger F., eds, AIP Conf. Proc. Vol. 1085, High Energy Gamma-Ray Astrology. Am. Inst. Phys., New York, p. 585
Gupta A. C., Banerjee D. P. K., Ashok N. M., Joshi U. C., 2004, A&A, 422, 505
Gupta A. C. et al., 2008, AJ, 136, 2359
Heidt J., Wagner S. J., 1996, A&A, 305, 42
Heidt J., Wagner S. J., 1998, A&A, 329, 853
Heidt J., Nilsson K., Sillanpää A., Takalo L. O., Pursimo T., 1999, A&A, 341, 683
Holder J. et al., 2003, ApJ, 583, L9
Horns D., Konopelko A., 2002, IAU Circular, 7907, 2
Hughes P. A., Aller H. D., Aller M. F., 1991, ApJ, 374, 57
Jang M., Miller H. R., 1997, AJ, 114, 565
Jannuzi B. T., Green R. F., French H., 1993, ApJ, 404, 100
Jannuzi B. T., Smith P. S., Elston R., 1994, ApJ, 428, 130
Krawczynski H., 2004, New Astron. Rev., 48, 367
Krawczynski H. et al., 2004, ApJ, 601, 151
Kurtanidze O. M., Nikolashvili M. G., 2002, in Giommi P., Massaro E., Palumbo G., eds, Blazar Astrophysics with *BeppoSAX* and Other Observatories. ASI Science Data Center, ESA-ESRIN, Frascati, p. 197
Kurtanidze O. M., Richter G. M., Nikolashvili M. G., 1999, in Raiteri C. M., Villata M., Takalo L. O., eds, Blazar Monitoring Towards the Third Millennium. Osservatorio Astronomico di Torino, Pino Torinese, p. 29
Ma L., Xie G. Z., Yi T. F., Zhou S. B., Li K. H., Zhang X., Dai H., 2010, Ap&SS, 327, 35
Mangalam A. V., Wiita P. J., 1993, ApJ, 406, 420
Marcha M., 1994, PhD dissertation, Univ. Manchester
Marscher A. P., 1996, in Miller H. R., Webb J. R., Noble J. C., eds, ASP Conf. Ser. Vol. 110, Blazar Continuum Variability. Astron. Soc. Pac., San Francisco, p. 248
Marscher A. P., Gear W. K., 1985, ApJ, 298, 114
Marscher A. P., Gear W. K., Travis J. P., 1992, in Valtaoja E., Valtonen M., eds, Variability of Blazars. Cambridge Univ. Press, Cambridge, p. 85
Miller H. R., Ferrara E. C., Daya A. B., Wilson J. W., Fried R. E., Noble J. C., Jang M., 1999, in Raiteri C. M., Villata M., Takalo L. O., eds, Blazar Monitoring Towards the Third Millennium. Osservatorio Astronomico di Torino, Pino Torinese, p. 20
Padovani P., Giommi P., 1995, ApJ, 444, 567
Perlman E. S. et al., 1996, ApJS, 104, 251
Perlman E. S. et al., 2006, in Miller H. R., Marshall K., Webb J. R., Aller M. F., eds, ASP Conf. Ser. Vol. 350, Blazar Variability Workshop II. Astron. Soc. Pac., San Francisco, p. 191
Qian S. J., Quirrenbach A., Witzel A., Krichbaum T. P., Hummel C. A., Zensus J. A., 1991, A&A, 241, 15
Rani B. et al., 2010, MNRAS, 404, 1992
Rani B., Gupta A. C., Joshi U. C., Ganesh S., Wiita P. J., 2011, MNRAS, 413, 2157
Romero G. E., 1995, Ap&SS, 234, 49
Romero G. E., Cellone S. A., Combi J. A., 1999, A&AS, 135, 477
Romero G. E., Cellone S. A., Combi J. A., Andruchow I., 2002, A&A, 390, 431
Sambruna R. M., Maraschi L., Urry C. M., 1996, ApJ, 463, 444
Schachter J. F. et al., 1993, ApJ, 412, 541
Sikora M., Madejski G., 2001, in Aharonian F. A., Völk H. J., eds, AIP Conf. Proc. Vol. 558, High Energy Gamma-Ray Astronomy. Am. Inst. Phys., New York, p. 275
Sol H., Pelletier G., Asseo E., 1989, MNRAS, 237, 411
Stalin C. S., Gopal-Krishna, Sagar R., Wiita P. J., 2004, MNRAS, 350, 175
Stetson P. B., 1987, PASP, 99, 191
Stetson P. B., 1992, J. R. Astron. Soc. Canada, 86, 71

Stocke J. T., Liebert J., Schmidt G., Gioia I. M., Maccacaro T., Schild R. E., Maccagni D., Arp H. C., 1985, ApJ, 298, 619

Stocke J. T., Morris S. L., Gioia I. M., Maccacaro T., Schild R. E., Wolter A., 1989, in Maraschi L., Maccacaro T., Ulrich M. H., eds, Lecture Notes in Physics, Vol. 334, BL Lac Objects. Springer, Berlin, p. 242

Tagliaferri G. et al., 2008, ApJ, 679, 1029

Tonello N., Kranich D., HEGRA collaboration, 2003, Int. Cosmic Ray Conf., 5, 2615

Urry C. M., Padovani P., 1995, PASP, 107, 803

Véron-Cetty M.-P., Véron P., 2006, A&A, 455, 773

Villata M., Raiteri C. M., Lanteri L., Sobrito G., Cavallone M., 1998, A&AS, 130, 305

Villata M., Raiteri C. M., Popescu M. D., Sobrito G., De Francesco G., Lanteri L., Ostorero L., 2000, A&AS, 144, 481

Villata M. et al., 2007, A&A, 464, L5

Wagner S. J., Witzel A., 1995, ARA&A, 33, 163

Xie G. Z., Zhou S. B., Dai B. Z., Liang E. W., Li K. H., Bai J. M., Xing S. Y., Liu W. W., 2002, MNRAS, 329, 689

This paper has been typeset from a TEX/LATEX file prepared by the author.